Original Article

Circular RNA_0001073 (*circ_0001073*) Suppresses The Progression of Non-Small Cell Lung Cancer via *miR-582-3p/RGMB* Axis

Xuefen Jing, M.D.[1#], Meiying Ren, M.D.[1#], Yongshun Fan, B.D.[2], Yuhua Fu, M.D.[1], Cuifeng Wang, M.D.[1*]

1. The First Affiliated Hospital of Baotou Medical College, Baotou, The Inner Mongolia Autonomous Region, China
2. Hohhot Kingmed Center for Clinical Laboratory, Hohhot, The Inner Mongolia Autonomous Region, China

Corresponding Address: The First Affiliated Hospital of Baotou Medical College, Baotou, The Inner Mongolia Autonomous Region, China
Email: rangqinyu8@163.com

#These authors contributed equally to this work.

Received: 18/November/2020, Accepted: 02/February/2021

Abstract

Objective: Reportedly, circular RNAs (circRNAs) exert a crucial regulatory role in cancer. *Circ_0001073* is derived from exons 3-5 of *ACVR2A* gene, which inhibits cancer progression. However, the role and mechanism of *circ_0001073* in non-small cell lung cancer (NSCLC) are unclear. This study aimed to explore the role and mechanism of *circ_0001073* in the development of NSCLC.

Materials and Methods: In this experimental study, microarray analysis was employed to filter differential expressed circRNAs in NSCLC tissues. Also, *circ_0001073*, microRNA-582-3p (*miR-582-3p*), and repulsive guidance molecule B (*RGMB*) mRNA expressions were examined by quantitative real-time polymerase chain reaction (qRT-PCR). NSCLC cell multiplication was measured by the cell counting kit-8 (CCK-8) assay. Scratch healing experiment and Transwell experiment were performed to assess cell migration and invasion, respectively. Flow cytometry was applied to analyze the apoptosis of NSCLC cells. Western blot was employed to assess RGMB protein expression. Additionally, dual-luciferase reporter gene experiment and RNA immunoprecipitation (RIP) experiment were applied to probe the binding sites between *miR-582-3p* and *circ_0001073* or *RGMB*.

Results: *Circ_0001073* was remarkably under-expressed in NSCLC tissues and cells. *Circ_0001073* overexpression impeded the multiplication, migration, and invasion and enhanced the apoptosis of NSCLC cells *in vitro*. *Circ_0001073* directly bound to *miR-582-3p* and acted as a miRNA sponge to regulate *RGMB* expression. Besides, *miR-582-3p* overexpression or knockdown of RGMB remarkably reversed the malignant phenotypes of NSCLC cells induced by the up-regulation of *circ_0001073* expression.

Conclusion: *Circ_0001073* up-regulates *RGMB* expression through adsorbing *miR-582-3p* to inhibit NSCLC progression, suggesting its potential as a novel therapeutic target in NSCLC.

Keywords: Circular RNA, MicroRNA, Non-Small Cell Lung Cancer, Repulsive Guidance Molecule B

Cell Journal(Yakhteh), Vol 23, No 6, November 2021, Pages: 684-691

Citation: **Jing XF, Ren MY, Fan YS, Fu YH, Wang CF. Circular RNA_0001073 (circ_0001073) suppresses the progression of non-small cell lung cancer via miR-582-3p/RGMB axis. Cell J. 2021; 23(6): 684-691. doi: 10.22074/cellj.2021.7872.**

Introduction

Lung cancer (LC) is a common and high-mortality disease and becomes the major cause of cancer-related deaths worldwide (1). Non-small cell lung cancer (NSCLC) is the main pathological type of LC, taking up 80-85% of all LC cases. Most patients with NSCLC are diagnosed at an advanced stage and suffer from an adverse prognosis, with a 5-year survival rate of less than 20% (2-4). It is imperative to discover novel and effective therapeutics for NSCLC.

Circular RNA (circRNA), an endogenous non-coding RNA molecule, is widely found in the eukaryotes. It has closed-loop structure and is more stable than linear RNA (5). CircRNAs are vital regulators in the development of diverse diseases, including cancers (6-11). For instance, *circ_0006332* expression is up-modulated in bladder cancer tissues, and it regulates *MYBL2* expression by working as a sponge for *miR-143*, thereby promoting bladder cancer progression (9). Reportedly, *circ_0001073* expression is down-modulated in the lung adenocarcinoma (LUAD) tissues compared with normal lung tissues (10). Nevertheless, whether *circ_0001073* regulates NSCLC progression remains largely unknown. Previous studies reported that *miR-582-3p* is abnormally expressed in different tumors, such as prostate cancer, acute myeloid leukemia, and NSCLC (12-14). A recent study reported that *miR-582-3p* enhances the cancer stem cell properties of NSCLC cells (14). However, the potential mechanism by which *miR-582-3p* regulates NSCLC has not been fully clarified.

Repulsive guidance molecule B (*RGMB*), also known as "*Dragon*", is the first discovered member of the RGM family (15). It is unveiled that *RGMB* expression is down-regulated in NSCLC, and knockdown of *RGMB* enhances the adhesion, migration, and invasion of NSCLC cells (16). This suggests that *RGMB* participates in the NSCLC progression as a tumor suppressor. Nonetheless, the

upstream regulatory mechanism of *RGMB* in NSCLC warrants further investigation.

In this work, we evaluated the expression profile of circRNAs in the NSCLC tissues and found that *circ_0001073* expression was markedly down-modulated in NSCLC tissues. We investigated the biological function of *circ_0001073* in NSCLC and its relationship with *miR-582-3p* and *RGMB*. The results suggested that *circ_0001073* suppressed the malignant phenotypes of NSCLC cells via regulating *miR-582-3p* and *RGMB*. This work provided new insights into the molecular mechanisms of NSCLC progression.

Materials and Methods

Clinical specimens

The research was endorsed by the Ethics Committee of the First Affiliated Hospital of Baotou Medical College (Baotou, China, 20180043) and written informed consent was obtained from all participating patients. Forty pairs of NSCLC tissues and paracancerous lung tissues were collected during surgery. Then, the tissue samples were frozen at -80°C. None of the subjects underwent radiotherapy or chemotherapy prior to the surgery. The experiments about human tissues were performed according to the Declaration of Helsinki.

Cell culture

LC cell lines [A549 (No. CCL-185), H460 (No. HTB-177), HCC827 (No. CRL-2868), H1299 (No. CRL-5803), and H1975 (No. CRL-5908)] and human bronchial epithelial cells (BEAS-2B, No.CRL-9609) from the American Type Culture Collection (ATCC, Rockville, MD, USA) were used in this study. All cells were maintained in RPMI-1640 medium (Cat No. 11875101, Gibco, Carlsbad, CA, USA) containing 10% fetal bovine serum (FBS, Cat No. 10099, Gibco, Carlsbad, CA, USA), 100 U/mL penicillin and 100 µg/mL streptomycin (Cat No. 15140163, Gibco, Carlsbad, CA, USA) at 37°C in 5% CO_2.

Cell transfection

The *circ_0001073* overexpression plasmid (pcDNA3.1-*circ_0001073*) was synthesized by GenePharma (Shanghai, China). Empty plasmid (pcDNA3.1-NC) was used as a negative control. siRNAs targeting *RGMB* (si-*RGMB*), *miR-582-3p* mimics, and the corresponding controls (si-NC and miR-con) were designed and synthesized by RiboBio (Guangzhou, China). Moreover, cells were transiently transfected using Lipofectamine 3000 (Invitrogen, Carlsbad, CA, USA) in line with the protocol.

Quantitative real-time polymerase chain reaction

Total RNA was separated from tissues and cells using TRIzol reagent (Cat No. 15596026, Invitrogen, Carlsbad, CA, USA) according to manufacturer's protocol. Then, 500 ng of total RNA was reversely transcribed into cDNA using Prime Script RT Master Mix (Cat No. RR036A, Takara, Dalian, China). Quantitative real-time polymerase chain reaction (qRT-PCR) was then executed on an ABI7500 system (ABI Biosystems, Foster City, CA, USA) with a Bestar™ qPCR Master Mix (Cat No. #2231, DBI Bioscience, Shanghai, China). Relative expression was calculated using the $2^{-\Delta\Delta Ct}$ method. The primer sequences selected in this research were as follows:

circ_0001073-

F: 5′-AAGATGGCCTACCCTCCTGT-3′
R: 5′-CCATAACACGGTTCAACACC-3′

RGMB−

F: 5′-GGCCTGGCCACTCATAGATA-3′
R:5′-ACTGAACCTGACCGTACATCATCTGTCACAG CTTGGTA-3′ (16)

GAPDH-

F:5′-GACTCATGACCACAGTCCATGC-3′
R: 5′-AGAGGCAGGGATGATGTTCTG-3′ (17)

miR-582-3p-

F: 5′-GCACACATTGAAGAGGACAGAC-3′
R: 5′-TATTGAAGGGGGTTCTGGTG-3′ (13)

U6-

F: 5′-CTCGCTTCGGCAGCACA-3′
R: 5′-AACGCTTCACGAATTTGCGT-3′(13)

β-actin-

F: 5′-CCTAGAAGCATTTGCGGTGG-3′
R: 5′-GAGCTACGAGCTGCCTGACG-3′

(Fig.S1, See Supplementary Online Information at www.celljournal.org).

RNase R assay

Total RNA was separated from A549 and H460 cells. Then, 5 µg of total RNA samples was incubated with 3 U/µg RNase R (Cat No. RNR07250, Epicenter Biotechnologies, Madison, WI, USA) for 20 minutes at 37°C. Subsequently, *circ_0001073* expression was determined by qRT-PCR, with *GAPDH* as a control.

Subcellular distribution experiment

Total RNA from the nuclei and cytoplasm of A549 and H460 cells was extracted using NE-PER Nuclear and Cytoplasmic Extraction Reagent (Cat No. 78835, Thermo Scientific, Waltham, MA, USA). qRT-PCR was applied to determine *circ_0001073* expression in the nuclei and cytoplasm, respectively. Besides, *U6* and *GAPDH* served as the nuclear and cytoplasmic controls, respectively.

Cell counting kit-8 experiment

Cell multiplication was detected using CCK-8 (Cat No. C0037, Beyotime, Shanghai, China). A549 and H460 cells were planted in 96-well plates (2×10^3 cells per well). At the specific time points (12, 24, 48, 72, and 96 h), 90 µL of serum-free medium and 10 µL of CCK-8

solution were supplemented to each well. The cells were then incubated at 37°C for 2 hours. Using Infinite M200 microplate reader (Tecan, Männedorf, Switzerland), the absorbance of the cells was determined at 450 nm.

Scratch-healing experiment

NSCLC cells were planted in 6-well plates and cultured. When the confluence reached 80-90%, the cells were scratched vertically with a pipette tip and rinsed twice with phosphate buffered solution (PBS), and the wound was observed under an inverted microscope, which was recorded as 0 h. After that, the cells were cultured with serum-free medium at 37°C in 5% CO_2, and the wound healing was observed at the same observation point after 24 hours. Scratch healing rate (%) was calculated based on below formula:

$$\text{Scratch healing rate (\%)} = \frac{\text{(0 h scratch width-24 h scratch width)}}{\text{(0 h scratch width)} \times 100}$$

Transwell experiment

Transwell chambers (Cat No. 3374, Corning, Shanghai, China) were used for migration and invasion assays. Only for invasion assay, we used Matrigel (Cat No. 356234, BD Biosciences, Franklin Lakes, NJ, USA). A549 and H460 cells (5×10^4 cells) in serum-free medium was added to the top compartment of chamber, and medium containing 10% FBS was supplemented to the bottom of it. After 24 hours culturing at 37°C, 5% CO_2, the upper membrane surface cells were swabbed with a cotton swab, and the migrating or invading cells were fixed with 95% ethanol (Cat No. 400203, Sigma-Aldrich, Louis, MO, USA) and stained with 0.2% crystal violet solution (Cat No. V5265, Sigma-Aldrich, Louis, MO, USA). Finally, the below membrane surface cells was counted under an optical microscope (Nikon, Tokyo, Japan).

Flow cytometry

Apoptosis was determined using the Annexin V-FITC apoptosis assay kit (Cat No. BMS500FI-300, Invitrogen, Carlsbad, CA, USA). A549 and H460 cells were trypsinized and rinsed with cold PBS. Subsequently, NSCLC cells (1×10^5 cells) were resuspended in 100 µL of binding buffer. After 20 minutes of incubation with 5 µL of Propidium iodide (PI) and 5 µL of Annexin V-FITC, apoptotic cells were immediately analyzed by a flow cytometry (BD Biosciences, San Jose, CA, USA).

Western blot

Extracting total protein, RIPA lysis buffer (Cat No. P0013C, Beyotime, Shanghai, China) was used, and protein concentration was examined following the manufacture's instruction of BCA protein assay kit (Cat No. #5000006, BioRad, Hercules, CA, USA). A total of 20 µg of protein was separated using sodium dodecyl sulfate-polyacrylamide gel electrophoresis (SDS-PAGE) and then transferred to PVDF membranes (Cat No. IPVH00010, Millipore, Bedford, MA, USA). After 1 hour blocking with 5% skim milk, the membranes were incubated with the following primary antibodies overnight at 4°C: anti-*RGMB* (Cat No. ab96727, Abcam, Shanghai, China, 1:1000) and anti-*GADPH* (Cat No. ab9485, Abcam, Shanghai, China, 1:1000). Then, the membranes were rinsed with TBST (Cat No. T1085, Solarbio, Beijing, China) and incubated with HRP-coupled goat anti-rabbit secondary antibody (Cat No. ab6721, Abcam, Shanghai, China, 1:2000) for 2 hours at room temperature. The protein bands were examined with the ECL Plus assay kit (Pierce, Rockford, IL, USA), and protein expression was quantified using Image-Pro Plus 6.0 software (Media Cybernetics, Bethesda, MD, USA).

RNA immunoprecipitation experiment

The RNA binding protein immunoprecipitation (RIP) assay was performed using the Magna RIP Kit (Cat No. 17-700, Millipore, Bedford, MA, USA) according to the manufacturer's protocols. Then, 1×10^7 precipitated cells were resuspended in a solution containing RIP lysis buffer, protease and RNase inhibitors. Also, 100 mL cell lysate was incubated with anti-Ago2 antibody (Cat No. Ab186733, Abcam, Shanghai, China) or immunoglobulin G (IgG; Cat No. MA5-27548, Millipore, Bedford, MA, USA) antibody overnight at 4°C. Immunoprecipitated RNA was isolated using the RNeasy MinElute Cleanup Kit (Cat No. 74204, Qiagen, Shanghai, China). Then reverse transcription was performed by Golden-star™ RT6 cDNA Synthesis Kit (according to the manufacturer's protocols) (Cat No. TSK302M, TSINGKE, Beijing, China). The immunoprecipitated RNA was detected by qRT-PCR to detect the abundance of *circ_0001073* and *miR-582-3p*.

Dual-luciferase reporter gene experiment

Synthesized sequences of *circ_0001073*, *RGMB* 3′-UTR and wild-type or mutant *miR-582-3p* binding sites were cloned into the psi-CHECK2 vector (Promega, Madison, WI, USA). Subsequently, luciferase vector and *miR-582-3p* mimics (or miR-con) were co-transfected into A549 and H460 cells using Lipofectamine 3000 (Invitrogen, Carlsbad, CA, USA). After 48 hours of transfection, luciferase activity was measured by using dual-luciferase assay system (Promega, Madison, WI, USA).

Statistical analysis

Various statistical analyses were performed by SPSS software version 20.0 (IBM Corp., Armonk, NY, USA). Students t test was used to compare the differences between two groups. Comparisons among multiple groups were analyzed by one-way ANOVA followed by a post hoc Tukey test for multiple comparisons. Pearson's correlation test was used to determine the relationships among *circ0001073*, *miR-582-3p*, and *RGMB* mRNA expressions $P<0.05$ signified statistical significance.

Results

Circ_0001073 was lowly expressed in NSCLC tissues and cells

Analyzing public dataset GSE112214 of microarray data, *circ_0001073* expression was down-modulated in NSCLC

tissues in compare with paracancerous tissues (Fig.1A) that were validated with qRT-PCR results (Fig.1B). In comparison with 16HBE cell line *circ_0001073* was significantly under-expressed in the NSCLC cell lines (Fig.1C). Furthermore, bioinformatics analysis uncovered that *circ_0001073* was an exonic circRNA consisting of three exons (exons 3, 4, and 5) of *ACVR2A* gene (Fig.1D) (18). RNase R assay indicated that *circ_0001073* was resistant to RNase R digestion, while *GAPDH* mRNA was sensitive (Fig.1E). Additionally, subcellular distribution analysis signified that *circ_0001073* was predominantly located in the cytoplasm of NSCLC cells (Fig.1F). We observed that the NSCLC patients with higher expression level of *circ_0001073* had a longer survival time compared with the patients with lower expression level of *circ_0001073* (Fig.1G).

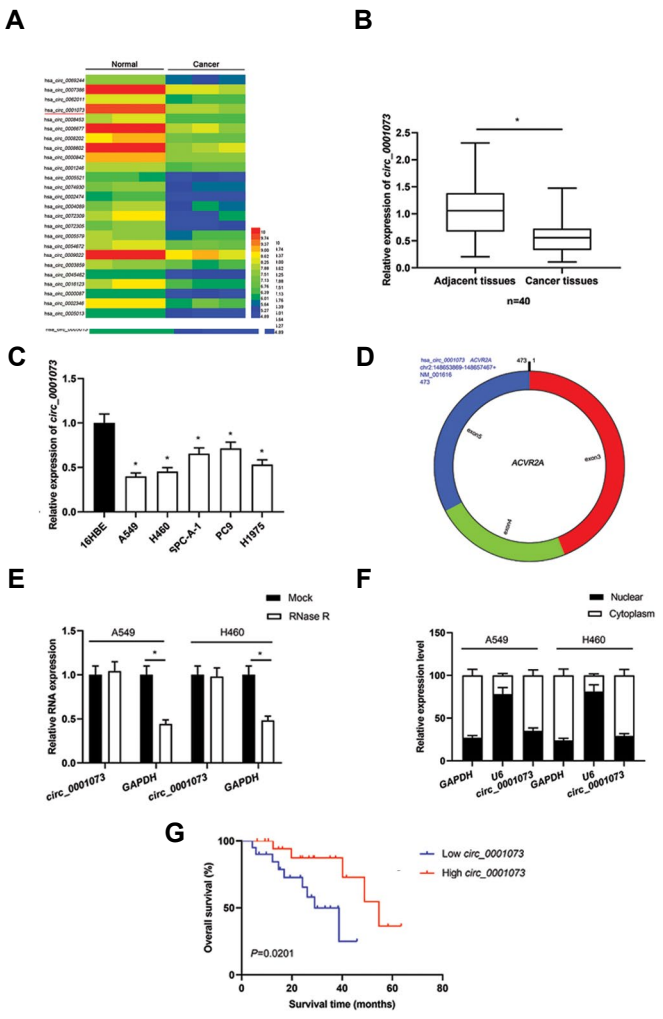

Fig.1: *Circ_0001073* expression in NSCLC tissues and cells. **A**. In dataset GSE112214, *circ_0001073* expression was significantly down-regulated in NSCLC tissues compared with paracancerous tissues. **B.** *Circ_0001073* expression in NSCLC tissues and paracancerous tissues was detected by qRT-PCR. **C.** *Circ_0001073* expression in NSCLC cells and 16HBE cells was detected by qRT-PCR analysis. **D.** The schematic diagram of the formation of *circ_0001073* from *ACVR2A* exons. **E.** The extracted RNA was treated with RNase R, and then the expression levels of *circ_0001073* and *GAPDH* mRNA were determined by qRT-PCR to determine the circular structure of *circ_0001073*. **F.** The expressions of *circ_0001073*, *U6* mRNA and *GAPDH* mRNA in the nuclei and cytoplasm of NSCLC cells were detected by qRT-PCR. **G.** Kaplan-Meier method was used to compare the survival time of the patients with high or low expression of *circ_0001073*. All experiments were performed in triplicate. *; P<0.05, NSCLC; Non-small cell lung cancer, and qRT-PCR; Quantitative real-time polymerase chain reaction.

Circ_0001073 overexpression restrained the multiplication, migration, and invasion of NSCLC cells and enhanced the apoptosis

To elaborate on the effects of *circ_0001073* on the proliferation, migration and invasion of NSCLC cells, *circ_0001073* overexpression plasmids were selected to be transfected into A549 and H460 cells with the lowest *circ_0001073* expression. The result of overexpression efficiency was illustrated in Figure 2A that has achieved by 48 hours after the transfection qRT-PCR. The multiplication of cells was examined by CCK-8 experiment. The results indicated that *circ_0001073* overexpression significantly inhibited the multiplication of A549 and H460 cells of NC group (Fig.2B). The data of scratch-healing experiments and Transwell experiments demonstrated that the cell migration and invasion in the *circ_0001073* overexpression group were significantly decreased compared with NC group (Fig.2C-H). Additionally, flow cytometry analysis manifested that *circ_0001073* overexpression significantly promoted the apoptosis of NSCLC cells (Fig.2I-J).

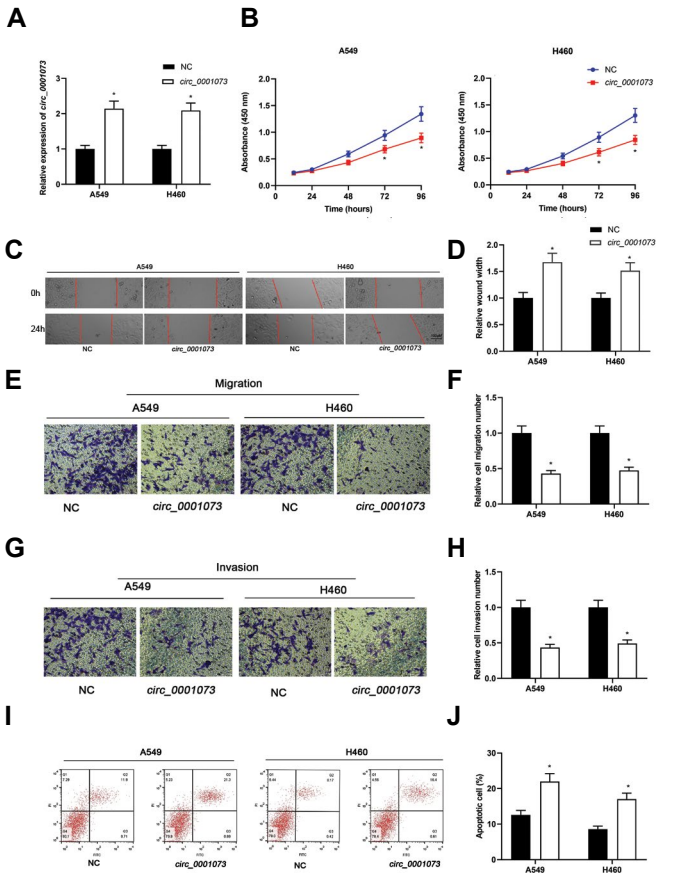

Fig.2: *Circ_0001073* overexpression inhibited the multiplication, migration, and invasion of NSCLC cells, and induced apoptosis. **A.** Using qRT-PCR analysis, *circ_0001073* expression was detected in the A549 and H460 cells after *circ_0001073* overexpression. **B.** After the transfection, cell multiplication was assessed using the CCK-8 method. **C, D.** Cell migration was assessed by wound-healing experiments. **E-H.** Transwell experiments were used to detect cell migration and invasion of NSCLC cells. **I, J.** Flow cytometry was used to detect apoptosis of NSCLC cells. All experiments were performed in triplicate. *; P<0.05, NC; Negative control, NSCLC; Non-small cell lung cancer, and qRT-PCR; Quantitative real-time polymerase chain reaction.

Circ_0001073 acted as a molecular sponge for *miR-582-3p* in NSCLC cells

Also, circRNAs mainly located in the cytoplasm, which has suggested that usually function as sponges for miRNAs (19). To pinpoint the underlying mechanism of circ_0001073 in the NSCLC, target miRNAs of *circ_0001073* were predicted by bioinformatic analysis tools (the result is available upon request). A complementary binding sequence was discovered between *circ_0001073* and *miR-582-3p* (Fig.3A). To validate the targeting relationship between them, dual-luciferase reporter gene experiment was conducted. In the A549 and H460 cells, data implied that high expression of *miR-582-3p* represses the luciferase activity of *circ_0001073*-WT, while had not any effect on *circ_0001073*-MUT (Fig.3B). RIP assay showed that *circ_0001073* and *miR-582-3p* were significantly enriched in the Ago2 group of A549 and H460 cells (Fig.3C). Moreover, *circ_0001073* overexpression significantly decreased *miR-582-3p* expression in A549 and H460 cells, indicating that *miR-582-3p* expression was regulated by *circ_0001073* (Fig.3D). We observed that *miR-582-3p* was significantly higher expressed in NSCLC tissues and cells compared with paracancerous tissues or 16HBE cells (Fig.3E, F). Correlation analysis showed a negative correlation between *miR-582-3p* expression and *circ_0001073* expressions in the NSCLC tissues (Fig.3G). The above data confirmed that *circ_0001073* could sponge *miR-582-3p* and inhibit its expression.

RGMB was a downstream target gene of *miR-582-3p*

Using the StarBase database, potential target genes of *miR-582-3p* were predicted that may elucidate the downstream mechanism of the *circ_0001073*/*miR-582-3p* axis in NSCLC (the result is available on request). A complementary binding sequence was discovered between *miR-582-3p* and *RGMB* 3´UTR, that was shown in Figure 4A. Dual-luciferase reporter experiments confirmed that *miR-582-3p* overexpression remarkably inhibits the luciferase activity of *RGMB*-WT in A549 and H460 cells whereas it exerts no significant effect on the luciferase activity of *RGM*B-MUT (Fig.4B). Moreover, qRT-PCR analysis showed that *miR-582-3p* expression was remarkably up-regulated in A549 and H460 cells transfected with *miR-582-3p* mimics (Fig.4C). The data of qRT-PCR and Western blot reveals that *miR-582-3p* overexpression remarkably inhibits *RGMB* mRNA and protein expression in NSCLC cells relative to the miR-con group (Fig.4D, E). Additionally, *RGMB* mRNA expression was remarkably down-modulated in NSCLC tissues and cells (Fig.4F, G). Correlation analysis showed that *RGMB* mRNA expression was negatively correlated with *miR-582-3p* expression and positively associated with *circ_0001073* expression in NSCLC tissues (Fig.4H, I). Furthermore, *RGMB* mRNA and protein expressions were remarkably down-regulated in the si-*RGMB* transfected cells. Since si-*RGMB*#1 had the highest knockdown efficiency (Fig.4J, K), therefore, we selected it for our subsequent experiments.

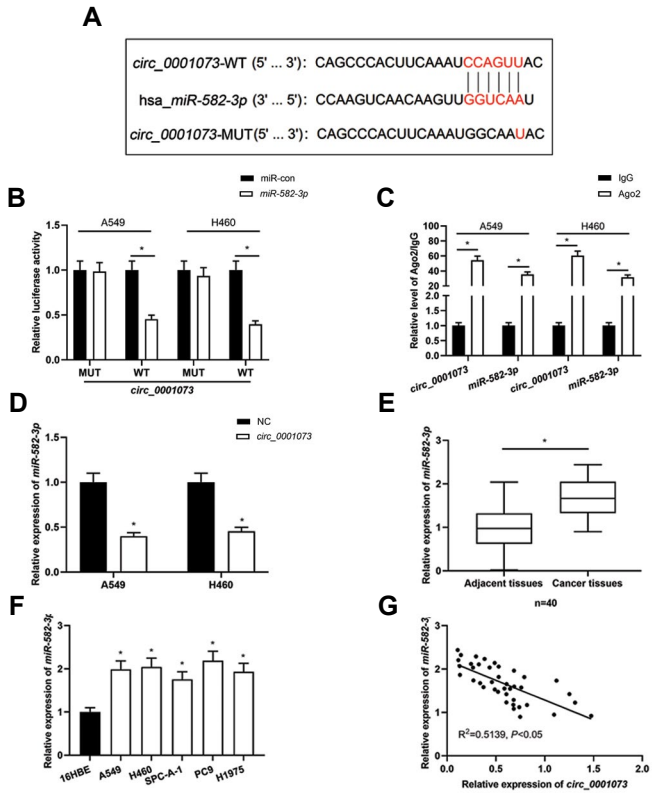

Fig.3: *MiR-582-3p* was the target of *circ_0001073*. **A.** Bioinformatics analysis predicted the binding sequence between *miR-582-3p* and *circ_0001073*. **B.** Dual-luciferase reporter gene experiments were used to verify the binding relationship between *miR-582-3p* and *circ_0001073*. **C.** The enrichment of *circ_0001073* and *miR-582-3p* in Ago2 or IgG immunoprecipitate was determined using the RIP method. **D.** *MiR-582-3p* expression in the *circ_0001073* overexpression plasmid transfected cells was detected by qRT-PCR analysis. **E, F.** Using qRT-PCR, *MiR-582-3p* expression was detected in the NSCLC tissues and cells. **G.** Pearson's correlation analysis was employed to analyze the correlation between *miR-582-3p* expression and *circ_0001073* expression in the NSCLC tissues. All experiments were performed in triplicate. *; P<0.05, NC; Negative control, NSCLC; Non-small cell lung cancer, and qRT-PCR; Quantitative real-time polymerase chain reaction.

Circ_0001073 up-regulated *RGMB* expression by targeting *miR-582-3p* to inhibit NSCLC progression

qRT-PCR and Western blot analysis showed that overexpression *circ_0001073* remarkably increased *RGMB* expression, while *miR-582-3p* mimics or si-*RGMB*#1 transfection reduced this phenomenon (Fig.5A, B). We observed that *miR-582-3p* mimics or si-*RGMB*#1 weakened the effects of *circ_0001073* overexpression on the multiplication, migration, and invasion of A549 and H460 cells (Fig.5C-F). Furthermore, flow cytometry analysis revealed that the promotion of apoptosis by *circ_0001073* overexpression could be attenuated by *miR-582-3p* mimics or si-*RGMB*#1 (Fig.5G). The above results indicated that the *miR-582-3p*/*RGMB* axis is vital for maintaining the function of *circ_0001073* in NSCLC cells.

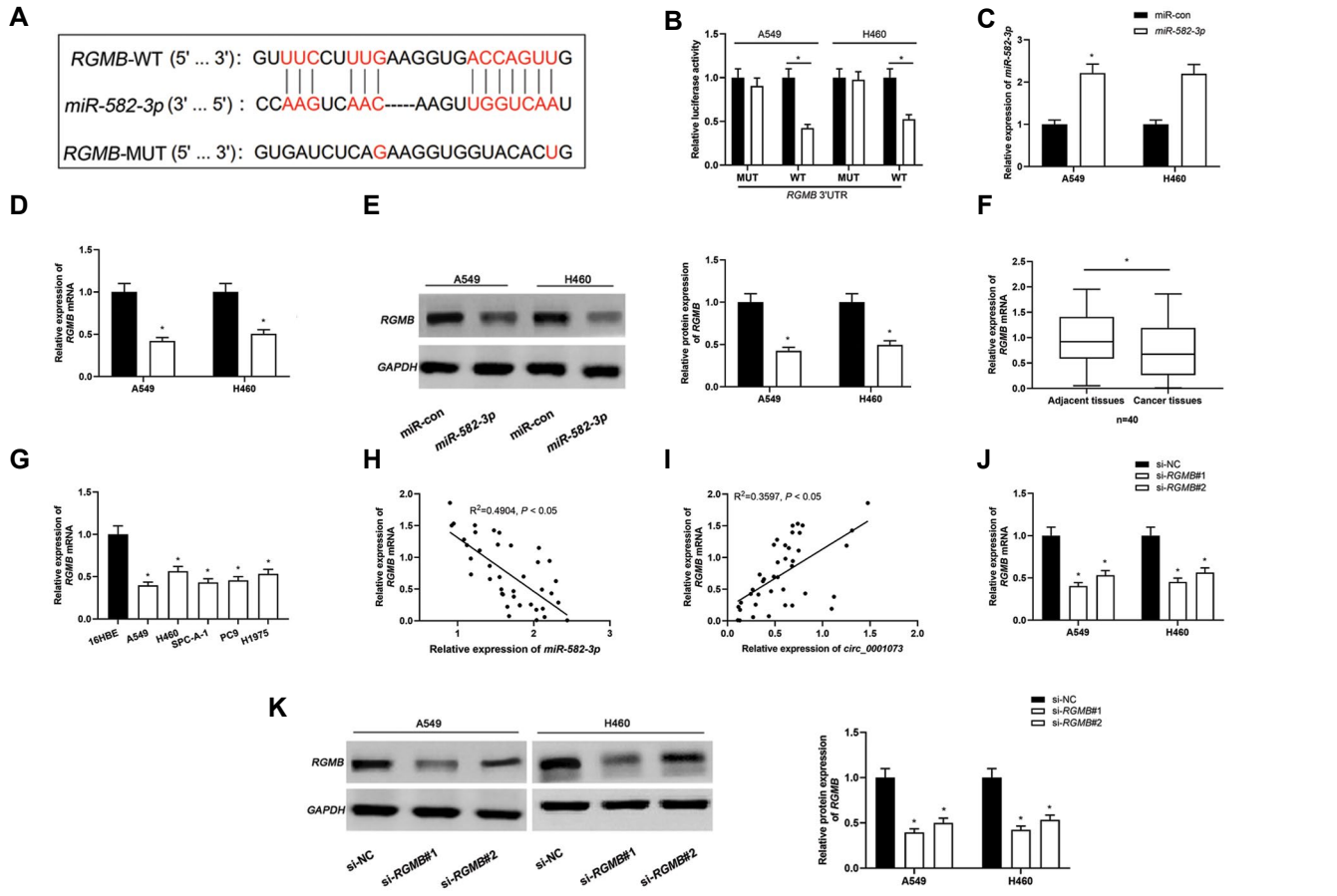

Fig.4: *RGMB* was a downstream target of *miR-582-3p* in NSCLC cells. **A.** Bioinformatics analysis predicted the binding sequence between *miR-582-3p* and *RGMB* 3´UTR. **B.** The binding relationship between *miR-582-3p* and *RGMB* was detected using the dual-luciferase reporter gene assay. **C.** qRT-PCR analysis was used to detect *miR-582-3p* expression in A549 and H460 cells after the transfection with *miR-582-3p* mimics. **D, E.** The *RGMB* expressions (mRNA and protein) in A549 and H460 cells transfected with *miR-582-3p* mimics were detected using qRT-PCR and Western blot. **F, G.** Using qRT-PCR, mRNA expression of *RGMB* was detected in NSCLC tissues and cells. **H, I.** Pearson's correlation analysis was used to analyze the correlation between *RGMB* mRNA and *miR-582-3p* or *circ_0001073* expression in NSCLC tissues. **J, K.** *RGMB* expression (mRNA and protein) in si-*RGMB* transfected cells (A549 and H460) was detected by qRT-PCR analysis and Western blot. All experiments were performed in triplicate. *; P<0.05, NSCLC; Non-small cell lung cancer, and qRT-PCR; Quantitative real-time polymerase chain reaction.

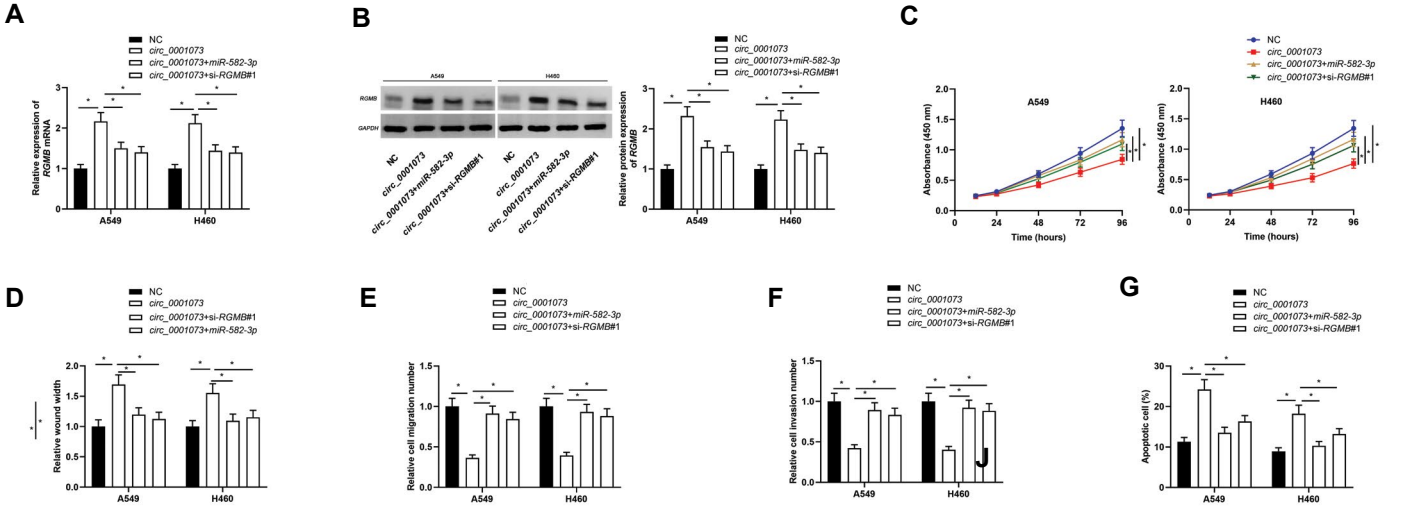

Fig.5: *Circ_0001073* modulated NSCLC progression via the *miR-582-3p/RGMB axis.* **A, B.** *RGMB* mRNA and protein expression was determined by qRT-PCR and Western blot. **C.** Cell multiplication was assessed using the CCK-8 method. **D.** Cell migration was assessed by wound-healing experiment. **E, F.** Transwell experiments were used to detect cell migration and invasion. **G.** Flow cytometry was used to detect the apoptosis of NSCLC cells. All experiments were performed in triplicate. *; P<0.05, NC; Negative control, NSCLC; Non-small cell lung cancer, and qRT-PCR; Quantitative real-time polymerase chain reaction.

Discussion

CircRNAs exhibit unique expression pattern and specific function in tumor progression (20, 21). Several lines of evidences have indicated that, aberrant circRNA expression is associated with the tumorigenesis and progression of NSCLC. For instance, *circ_0000376*

expression is up-regulated in the NSCLC tissues; *circ_0000376* overexpression promotes the multiplication and metastasis of the NSCLC cells and enhances their chemoresistance (22). In contrast, *circ_0002483* is under-expressed in NSCLC tissues and cell lines, which inhibits NSCLC progression by targeting *miR-182-5p* and enhances the sensitivity of cancer cells to paclitaxel (23). Some studies have shown that *circ_0001073* is under-expressed in bladder cancer and breast cancer (24, 25). *Circ_0001073* overexpression restrains the multiplication and metastasis of bladder cancer cells (24). Moreover, the down-modulation of *circ_0001073* expression is linked to the unfavorable breast cancer prognosis in these patients, and *circ_0001073* overexpression inhibits breast cancer cell multiplication and induces apoptosis (25). Our result confirmed that *circ_0001073* expression was markedly down-modulated in NSCLC tissues and cells and *circ_0001073* overexpression impeded the multiplication, migration, and invasion of NSCLC cells and induced apoptosis. Our results suggested that *circ_0001073* was a tumor suppressor in NSCLC.

CircRNAs can participate in regulating cancer development by functioning as miRNA sponges to modulate miRNA expression (26). For instance, *circ_0026134* enhances the multiplication and invasion of NSCLC cells by sponging *miR-1256* and *miR-1287* (27). *Circ_ZNF124* activates the *JAK2/STAT3* signaling pathway by targeting *miR-337-3p*, thereby promotes NSCLC development (28). In this work, *circ_0001073* was confirmed to act as a molecular sponge for *miR-582-3p* and negatively regulator of *miR-582-3p* expression in the NSCLC cells. The biological functions of *miR-582-3p* are investigated in many cancers. Huang et al. (12), reported that, *miR-582-3p* and *miR-582-5p* inhibit bone metastasis of prostate cancer by impeding TGF-β signaling; also, Li et al. (13), observed that *miR-582-3p* negatively modulates the multiplication and cell cycle progression of acute myeloid leukemia cells by targeting cyclin B2. Importantly, *miR-582-3p* exerts a carcinogenic effect in NSCLC: it inhibits the apoptosis of A549, NCI-H1703, and NCI-H1975 cells, and enhances their stem cell properties (14). Consistently, the present study confirmed that *miR-582-3p* was remarkably overexpressed in NSCLC tissues and cell lines. In addition, *miR-582-3p* markedly counteracted the effects of *circ_0001073* multiplication, migration, invasion, and apoptosis of the NSCLC cell. The above data implied that *circ_0001073* could exert tumor-suppressive effects in NSCLC progression by targeting *miR-582-3p*.

RGMB, a member of RGM family, is a regulator in the regeneration and remodeling of axons and synapses and a co-receptor for bone morphogenetic protein (BMP) (29-31). Also, RGM family included *RGMA*, *RGMB*, and *RGMC* (29). *RGMB* can directly interact with the BMP receptors of *BMP-2* and *BMP-4*, thereby augmenting the binding to ligands (31). Involvement in the BMP signaling pathway, *RGMB* is implicated in cancer initiation and development (32). Reportedly, *RGMB* expression is up-regulated in the colorectal cancer tissues, that subsequently, inhibits oxaliplatin-induced phosphorylation of *JNK* and *p38 MAPK* and reduces oxaliplatin-induced apoptosis (33). In squamous cell carcinoma of the head and neck, *RGMB*, targeted by *miR-93-5p*, participates in regulating the migration and invasion of tumor cells (34). Importantly, *RGMB* inhibits NSCLC progression via regulating Smad1/5/8 pathway (16). Notably, the present work revealed that *RGMB* expression is down-modulated in the NSCLC tissues and cells. Additionally, *RGMB* was confirmed to be a downstream target gene of *miR-582-3p*, and *RGMB* expression was negatively correlated with *miR-582-3p* expression and positively associated with *circ_0001073* expression in NSCLC tissues. What's more, transfection of *miR-582-3p* mimics or si-*RGMB* remarkably reversed the suppressive effects of *circ_0001073* on NSCLC cell multiplication, migration, and invasion and apoptosis promotion. These demonstrations suggest that the *circ_0001073*/*miR-582-3p*/*RGMB* axis was present in the NSCLC.

Collectively, this study found that the expression of *circ_0001073* was down-regulated in the NSCLC tissues and cells that participates in regulating the proliferation, migration, invasion, and apoptosis of NSCLC cells by modulating *miR-582-3p*/*RGMB* axis. To our knowledge, this is the first report to reveal the interactions among *circ_0001073*, *miR-582-3p* and *RGMB* in the NSCLC. However, our demonstrations are only based on in *vitro* assays, and the conclusions should be validated by *in vivo* research in the following studies. In the future, studies will be concentrated on, the identification of other *circ_0001073* downstream miRNAs.

Conclusion

This study elucidates that *circ_0001073* up-regulates *RGMB* expression by targeting *miR-582-3p* that associated with inhibiting the proliferation, migration, and invasion of NSCLC cells and inducing cell apoptosis. This study reveals a new molecular mechanism in the progression of NSCLC and provides new insights into the treatment of NSCLC.

Acknowledgments

We thank Hubei Yican Health Industry Co., Ltd. for its linguistic assistance during the preparation of this manuscript. The data used to support the findings of this study are available from the corresponding author upon request. The authors declare that they have no competing interests.

Authors' Contributions

C.W.; Conceive and experiments design. X.J., M.R.,

Yo.F., Yu.F.; Experiments performing. Yo.F., Yu.F.; Data analysis. X.J., M.R., Yo.F., Yu.F.; Manuscript writing. All authors read and approved the final manuscript.

References

1. Siegel RL, Miller KD, Jemal A. Cancer statistics, 2018. CA Cancer J Clin. 2018; 68(1): 7-30.
2. Hirsch FR, Scagliotti GV, Mulshine JL, Kwon R, Curran WJ Jr, Wu YL, et al. Lung cancer: current therapies and new targeted treatments. Lancet. 2017; 389(10066): 299-311.
3. Mao Y, Yang D, He J, Krasna MJ. Epidemiology of lung cancer. Surg Oncol Clin N Am. 2016; 25(3): 439-445.
4. Tan S, Gou Q, Pu W, Guo C, Yang Y, Wu K, et al. Circular RNA F-circEA produced from EML4-ALK fusion gene as a novel liquid biopsy biomarker for non-small cell lung cancer. Cell Res. 2018; 28(6): 693-695.
5. Yang M, Wang GY, Qian H, Ji XY, Liu CY, Zeng XH, et al. Circ-CCDC66 accelerates proliferation and invasion of gastric cancer via binding to miRNA-1238-3p. Eur Rev Med Pharmacol Sci. 2019; 23(10): 4164-4172.
6. Liu T, Song Z, Gai Y. Circular RNA circ_0001649 acts as a prognostic biomarker and inhibits NSCLC progression via sponging miR-331-3p and miR-338-5p. Biochem Biophys Res Commun. 2018; 503(3): 1503-1509.
7. Yin GH, Gao FC, Tian J, Zhang WB. Hsa_circ_101882 promotes migration and invasion of gastric cancer cells by regulating EMT. J Clin Lab Anal. 2019; 33(9): e23002.
8. Legnini I, Di Timoteo G, Rossi F, Morlando M, Briganti F, Sthandier O, et al. Circ-ZNF609 is a circular RNA that can be translated and functions in myogenesis. Mol Cell. 2017; 66(1): 22-37. e9.
9. Li M, Liu Y, Liu J, Li W, Li N, Xue D, et al. Circ_0006332 promotes growth and progression of bladder cancer by modulating MYBL2 expression via miR-143. Aging (Albany NY). 2019; 11(22): 10626-10643.
10. Zhang L, Ding F. Hsa_circ_0008945 promoted breast cancer progression by targeting miR-338-3p. Onco Targets Ther. 2019; 12: 6577-6589.
11. Li Y, Hu J, Li L, Cai S, Zhang H, Zhu X, et al. Upregulated circular RNA circ_0016760 indicates unfavorable prognosis in NSCLC and promotes cell progression through miR-1287/GAGE1 axis. Biochem Biophys Res Commun. 2018; 503(3): 2089-2094.
12. Huang S, Zou C, Tang Y, Wa Q, Peng X, Chen X, et al. miR-582-3p and miR-582-5p suppress prostate cancer metastasis to bone by repressing TGF-β signaling. Mol Ther Nucleic Acids. 2019; 16: 91-104.
13. Li H, Tian X, Wang P, Huang M, Xu R, Nie T. MicroRNA-582-3p negatively regulates cell proliferation and cell cycle progression in acute myeloid leukemia by targeting cyclin B2. Cell Mol Biol Lett. 2019; 24: 66.
14. Fang L, Cai J, Chen B, Wu S, Li R, Xu X, et al. Aberrantly expressed miR-582-3p maintains lung cancer stem cell-like traits by activating Wnt/β-catenin signalling. Nat Commun. 2015; 6: 8640.
15. 15. Shi Y, Huang XX, Chen GB, Wang Y, Zhi Q, Liu YS, et al. Dragon (RGMb) induces oxaliplatin resistance in colon cancer cells. Oncotarget. 2016; 7(30): 48027-48037.
16. Li J, Ye L, Shi X, Chen J, Feng F, Chen Y, et al. Repulsive guidance molecule B inhibits metastasis and is associated with decreased mortality in non-small cell lung cancer. Oncotarget. 2016; 7(13): 15678-15689.
17. Xu J, Ding R, Xu Y. Effects of long non-coding RNA SPRY4-IT1 on osteosarcoma cell biological behavior. Am J Transl Res. 2016; 8(12): 5330-5337.
18. Zhong S, Wang J, Zhang Q, Xu H, Feng J. CircPrimer: a software for annotating circRNAs and determining the specificity of circRNA primers. BMC Bioinformatics. 2018; 19(1): 292.
19. Chen LL. The biogenesis and emerging roles of circular RNAs. Nat Rev Mol Cell Biol. 2016; 17(4): 205-211.
20. Chen Q, Zhang J, He Y, Wang Y. hsa_circ_0061140 knockdown reverses FOXM1-mediated cell growth and metastasis in ovarian cancer through miR-370 sponge activity. Mol Ther Nucleic Acids. 2018; 13: 55-63.
21. Yang C, Yuan W, Yang X, Li P, Wang J, Han J, et al. Circular RNA circ-ITCH inhibits bladder cancer progression by sponging miR-17/miR-224 and regulating p21, PTEN expression. Mol Cancer. 2018; 17(1): 19.
22. Sun H, Chen Y, Fang YY, Cui TY, Qiao X, Jiang CY, et al. Circ_0000376 enhances the proliferation, metastasis, and chemoresistance of NSCLC cells via repressing miR-384. Cancer Biomark. 2020; 29(4): 463-473.
23. Li X, Yang B, Ren H, Xiao T, Zhang L, Li L, et al. Hsa_circ_0002483 inhibited the progression and enhanced the Taxol sensitivity of non-small cell lung cancer by targeting miR-182-5p. Cell Death Dis. 2019; 10(12): 953.
24. Dong W, Bi J, Liu H, Yan D, He Q, Zhou Q, et al. Circular RNA ACVR2A suppresses bladder cancer cells proliferation and metastasis through miR-626/EYA4 axis. Mol Cancer. 2019; 18(1): 95.
25. Yi Z, Li Y, Wu Y, Zeng B, Li H, Ren G, et al. Circular RNA 0001073 attenuates malignant biological behaviours in breast cancer cell and is delivered by nanoparticles to inhibit mice tumour growth. Onco Targets Ther. 2020; 13: 6157-6169.
26. Dong Y, He D, Peng Z, Peng W, Shi W, Wang J, et al. Circular RNAs in cancer: an emerging key player. J Hematol Oncol. 2017; 10(1): 2.
27. Chang H, Qu J, Wang J, Liang X, Sun W. Circular RNA circ_0026134 regulates non-small cell lung cancer cell proliferation and invasion via sponging miR-1256 and miR-1287. Biomed Pharmacother. 2019; 112: 108743.
28. Li Q, Huang Q, Cheng S, Wu S, Sang H, Hou J. Circ_ZNF124 promotes non-small cell lung cancer progression by abolishing miR-337-3p mediated downregulation of JAK2/STAT3 signaling pathway. Cancer Cell Int. 2019; 19: 291.
29. Siebold C, Yamashita T, Monnier PP, Mueller BK, Pasterkamp RJ. RGMs: structural insights, molecular regulation, and downstream signaling. Trends Cell Biol. 2017; 27(5): 365-378.
30. Wang X, Cheng JL, Ran YC, Zhang Y, Yang L, Lin YN. Expression of RGMb in brain tissue of MCAO rats and its relationship with axonal regeneration. J Neurol Sci. 2017; 383: 79-86.
31. Liu J, Wang W, Liu M, Su L, Zhou H, Xia Y, et al. Repulsive guidance molecule b inhibits renal cyst development through the bone morphogenetic protein signaling pathway. Cell Signal. 2016; 28(12): 1842-1851.
32. Meng C, Liu W, Huang H, Wang Y, Chen B, Freeman GJ, et al. Repulsive guidance molecule b (RGMb) is dispensable for normal gonadal function in mice. Biol Reprod. 2016; 94(4): 78.
33. Shi Y, Chen GB, Huang XX, Xiao CX, Wang HH, Li YS, et al. Dragon (repulsive guidance molecule b, RGMb) is a novel gene that promotes colorectal cancer growth. Oncotarget. 2015; 6(24): 20540-20554.
34. Zhang S, He Y, Liu C, Li G, Lu S, Jing Q, et al. miR-93-5p enhances migration and invasion by targeting RGMB in squamous cell carcinoma of the head and neck. J Cancer. 2020; 11(13): 3871-3881.